Hysteresis in a light bulb: connecting electricity and thermodynamics with simple experiments and simulations

D A Clauss, R M Ralich and R D Ramsier

Department of Physics, University of Akron, Akron, OH 44325-4001, USA

E-mail: rex@uakron.edu

Abstract
A method for integrating energy conversion phenomena, nonlinear circuit behaviour and hysteresis into a simple laboratory activity is demonstrated. Current–voltage data for a flashlight bulb driven at various frequencies and amplitudes are measured and simulated. Non-ohmic behaviour and hysteresis are observed experimentally and reproduced numerically with a model that includes the temperature-dependent specific heat capacity and electrical resistivity of the filament. The phenomenological model and simple experimental design could be modified for a variety of audiences.

1. Introduction

Incandescent light bulbs, in addition to providing illumination, are useful in the context of teaching physics. They can be used as a visual means of detecting current distributions in electrical circuits [1, 2] and techniques using bulbs in this way have proven to be effective in the classroom [3, 4]. Light bulbs also offers a means of investigating the physical properties of materials through the temperature-dependent behaviour of the filament. For example, emissivity, electrical resistivity, heat capacity and vapour pressure are filament properties which have been discussed in the literature [5–10]. In addition, light bulbs have been used for stellar spectroscopy [11] and investigations of fluctuation phenomena [12]. The light bulb is particularly appealing as an educational tool since there is an abundance of information available [13–17] on materials of construction, design, and operating principles.

The present paper demonstrates how a light bulb can be used to investigate another important physical phenomenon, hysteresis. Hysteresis is observed in many physical systems (e.g. magnetic, superconducting, ferroelectric, mechanical, etc) and there have been efforts to develop mathematical models of this behaviour [18]. Here, current–voltage (I–V) curves are presented for a flashlight bulb driven at various frequencies and amplitudes with the goal of providing a simple physical model that closely reproduces the observed non-ohmic behaviour and hysteresis. To achieve this goal, several simplifying assumptions are made concerning the thermal properties of the filament, and its effective geometry and emissivity are treated as variable parameters. This approach is simple and can be modified for use with various

audiences as (1) a demonstration that can be easily observed by all students, (2) an experimental laboratory for students beginning science and engineering and (3) an advanced undergraduate modelling project.

2. Experimental arrangement

Current–voltage measurements are performed while applying a sinusoidal voltage (2–10 V amplitude, 0.01, 0.1, 1, 10 and 100 Hz frequencies) across a No. 50 flashlight bulb mounted on a Pasco [19] Scientific circuit board (RLC Circuit, CI-6512). The voltage across the bulb is recorded with a Pasco Science Workshop^{TM} 750 Interface and Science Workshop^{TM} Version 2.2 software. The Pasco power amplifier (CI-6552A) measures the current internally. Sampling rates are adjusted so that the same number of data points is taken for each frequency. Measurements are recorded when dynamic equilibrium has been reached after the initial transients. To verify that the behaviour observed in the I–V curves is not an artifact of the signal generator, the current through the circuit is verified independently with an ohmic resistor placed in series with the light bulb.

3. Phenomenological modelling

The tungsten filament is extremely brittle and attempts to accurately measure its actual geometry proved unsuccessful. Also, since the goal of this work is to reproduce the electrical and thermal behaviour of the filament and not its geometric properties, the model defines the geometry using some simple approximations. The filament is assumed to be a uniform cylinder of cross-sectional area A_c and length L. The assumption of uniformity neglects the possibility that a real filament has thin regions due to the mechanical processing needed to form the coil, as well as evaporation during use which effectively limits the useful lifetime of the bulb [9]. The assumption of a cylinder instead of a coil will overestimate the effective radiating area [6], since regions on the inside of the coil radiate back and forth, trapping some of the energy and resulting in higher filament temperatures than would be obtained with a straight cylinder. The volumetric thermal expansion of the filament only provides a correction of less than 1%, therefore the model considers the geometry as independent of temperature.

The electrical power into the filament includes the voltage (V) as a function of time (t) and the filament resistance (R) and heat capacity (C) as functions of absolute temperature (T). The surroundings are assumed to be at a constant room temperature T_0. The filament resistance is expressed in terms of the resistivity of tungsten $\rho(T)$ as

$$R(T) = \rho(T)L/A_c. \tag{1}$$

It then follows that

$$A_c = \rho_0 L / R_0 \tag{2}$$

can be used to define the filament geometry in terms of the room temperature values of resistance and resistivity, R_0 and ρ_0, respectively. This is then used to calculate the diameter and surface area of the filament. The heat capacity is then expressible in terms of the volumetric specific heat capacity (c) as

$$C(T) = c(T)LA_c = c(T)L^2\rho_0/R_0. \tag{3}$$

The basic approach is to balance the electrical power input to the bulb with the power output to yield

$$V^2(t)/R(T) = C(T)dT/dt + K(T)(T - T_0) + e\sigma A_s T^4 \tag{4}$$

where e and A_s represent the emissivity and surface area of the filament, respectively, and σ is the Stefan–Boltzmann constant. For the temperature range in this work it is reasonable to assume $T^4 \gg T_0^4$ and neglect absorption of radiation from the surroundings. The quantity

$K(T)$ represents the conductive and convective properties of the system. For low power vacuum bulbs, such as those used in this study, the literature indicates that convection and conduction are negligible [5, 7, 10]; and this has been verified in the present work. In light of these findings, it is also reasonable to neglect the term involving $K(T)$. With this simplification and equations (1)–(3), equation (4) reduces to

$$V^2(t)/\rho(T) = c(T)L^2 \mathrm{d}T/\mathrm{d}t + e\sigma(4\pi R_0/\rho_0)^{1/2}L^{3/2}T^4. \tag{5}$$

Data for $\rho(T)$ and $c(T)$ found in the literature [17] are interpolated using polynomial expressions. This simplified model treats e and L as temperature-independent variable parameters and results in a nonlinear differential equation which is solved for $T(t)$ numerically using a MatLab$^\copyright$ ODE solver [20]. This is then used to calculate $R(t)$ and, knowing the input $V(t)$, Ohm's law is used to calculate the current $I(t)$.

4. Results and discussion

Figure 1 presents experimental $I–V$ data for a bulb driven sinusoidally at an amplitude of 10 V. Non-ohmic behaviour at low frequency is gradually replaced by linear $I–V$ curves by 100 Hz (not shown). Hysteresis is minimal at both low and high frequencies, reaching a maximum at around 1 Hz. Note also that the region of hysteresis shifts from near the origin at low frequency to far from the origin at successively higher frequencies. In addition, for the 0.01, 0.1 and 1 Hz data sets, the elbows (i.e. the regions where the slope changes abruptly) occur when the voltage is increasing in magnitude as indicated by the inset arrows. Thus the regions where the voltage is increasing are more nonlinear than those where the voltage is decreasing, and highly symmetric with respect to the origin.

The results from the numerical model are plotted along with the experimental data in figure 1 and the agreement is excellent. The variable parameter values used in these simulations are $L = 3.7$ cm and $e = 0.35$. However, these values should only be interpreted as reasonable estimates and not as actual values of the filament length and emissivity. The value of L is the same order of magnitude as the estimated length (2.4 cm) approximated under an optical microscope. In addition, using $L = 3.7$ cm in equation (2) yields a filament diameter of 30 μm, which is the correct order of magnitude for low power bulbs [9, 21]. The value of e is also in good agreement with literature values for the average emissivity of tungsten filaments [5, 6]. Although the task of reproducing the electrical and thermal properties of the filament is accomplished in figure 1, it is reassuring that the assumptions included in the model result in physically reasonable values for L and e. Note the number of experimental data points plotted in each curve of figure 1 has been significantly reduced in order to illustrate that the model closely reproduces the intricate details found in the experimental data.

The data of figure 2 are collected at a fixed frequency of 1 Hz, corresponding to the region where the maximum amount of hysteresis is observed in figure 1, but for different amplitudes. These data indicate that the amount of hysteresis and nonlinearity increases with the amplitude of the driving voltage. Again note the symmetry with respect to the origin and the different behaviour for the increasing and decreasing regions of the voltage cycles as indicated by the arrows. For the calculated results of figure 2, the same parameter values discussed earlier are used and once again the model predictions are in excellent agreement with the experimental data. As in figure 1, the experimental data-point density has been limited in the plots of figure 2 for clarity. Together, figures 1 and 2 clearly indicate that the model captures the important details of the electrical and thermal behaviour of this system within the frequency and amplitude ranges studied.

Nonlinear behaviour is expected in this system, since the resistance of the filament changes with temperature and the temperature range is large. The frequency-dependent behaviour is less straightforward to interpret, but can be traced to variable heating and cooling rates of the filament. The origin of different heating and cooling rates can be seen by returning to equation (5) with the input power defined as $P_i \propto V^2$ and the output power as $P_0 \propto T^4$. The
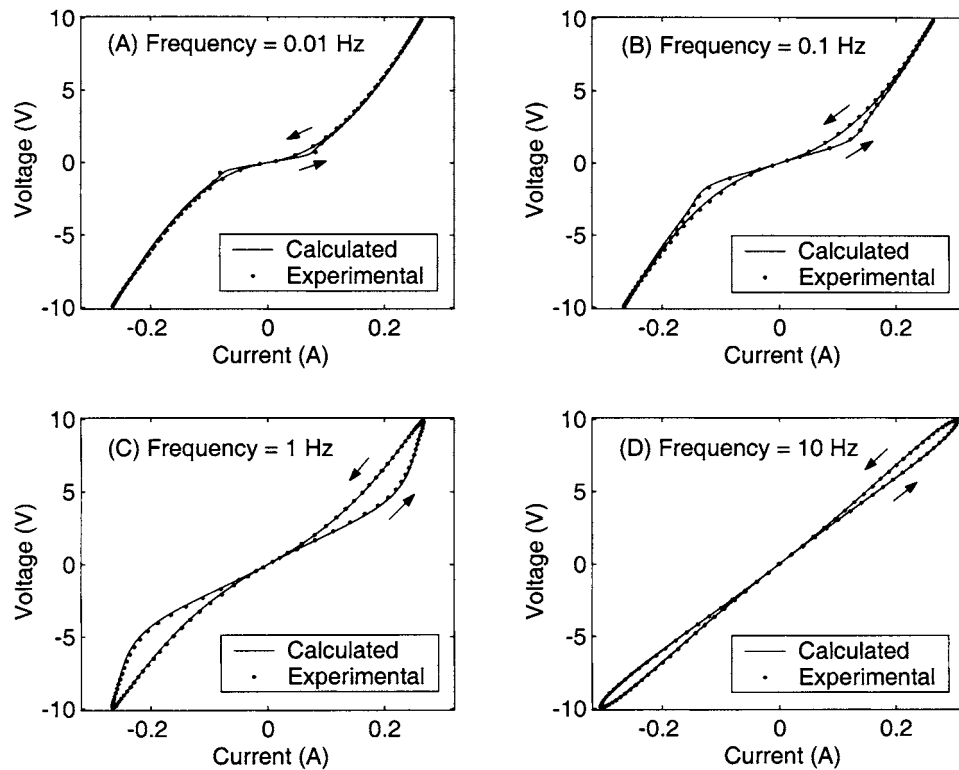
Figure 1. Measured and calculated I–V curves for the bulb driven at various frequencies with a constant amplitude (10 V) sine-wave. The inset arrows indicate the direction of increasing time.

rate $(\mathrm{d}T/\mathrm{d}t)$ is then proportional to the difference in power $(P_{\mathrm{i}} - P_0)$ and will therefore depend on the magnitude of the applied voltage and the temperature of the filament.

With hysteresis defined as the total area enclosed in a loop, figure 3 shows that the model predicts that the hysteresis will tend to zero at both low and high frequencies. The maximum amount of hysteresis occurs for the 10 V plot at a frequency of 3.2 Hz, corresponding to a period of 0.31 s. However, it is obvious that this value cannot be directly connected to a specific time constant of the filament alone since the locations of the maxima in figure 3 shift with amplitude. The scatter in the data at high frequency is due to step-size limitations in the numerical integration scheme and is not considered physically meaningful.

The accuracy of the model indicates that the behaviour of this filament is determined by its thermal properties. A simple way to understand how the thermal behaviour can cause hysteresis is to examine figure 1(c) at the locations where the applied voltage is 5 V. Letting the current where the voltage is increasing be I_i and the current where the voltage is decreasing be I_{d}, this I–V curve indicates that $I_{\mathrm{d}} < I_{\mathrm{i}}$ when the voltage is 5 V. The definition of resistance, $R = V/I$ implies there are two resistances, $R_{\mathrm{d}} > R_{\mathrm{i}}$, and therefore two temperatures, $T_{\mathrm{d}} > T_{\mathrm{i}}$. Hysteresis occurs during a cycle when there are different filament temperatures at the same applied voltage.

A closer analysis requires examining the solutions $T(t)$ of equation (5). The bold full curves of figure 4 are the complete solutions to equation (5) numerically calculated using the same parameter values given earlier for figure 1. To help understand these curves, figure 4 also includes approximate solutions to equation (5). With the rate-dependent term in equation (5) set equal to zero and using the approximate relation [6, 8–10] for tungsten $R \propto T^{1.2}$, equation (5)
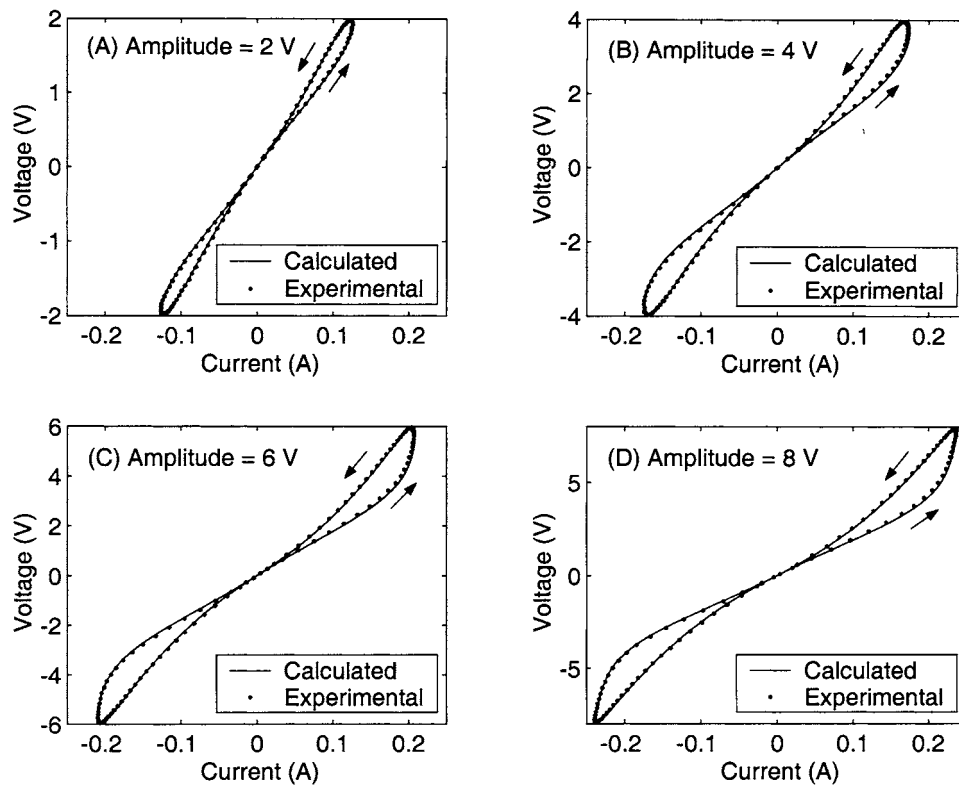
Figure 2. Measured and calculated I–V curves for the bulb driven at constant frequency (1 Hz) by a sine-wave of various amplitudes. The inset arrows indicate the direction of increasing time.

can be solved for $T(V)$ to yield $T \propto V^{0.38}$. This is then used in figure 4 to obtain the horizontal broken lines in which $V = V_{\text{rms}}$ (root-mean-squared voltage) and the thin full curves in which $V = V_0 \sin(2\pi f t)$ with $f =$ frequency and $V_0 =$ amplitude.

For sufficiently low frequencies the thermal response time of the filament is less than the period of the driving voltage (see the bottom section of figure 4). This allows near-equilibrium thermal conditions to be reached at each value of the sinusoidal input voltage, whether the voltage is increasing or decreasing. With no distinction between the increasing and decreasing parts of the cycle the hysteresis is minimized. Note that the small amount of hysteresis still present at low frequencies occurs when the sinusoidal voltage is near zero, as can also be seen in figure 1(a). The bottom plots of figure 4 indicate that the calculated temperature of the filament (bold curves) coincides with the thin lines at low frequencies demonstrating that the filament has sufficient time to react to the driving voltage.

For sufficiently high frequencies the thermal response time of the filament is greater than the period of the driving voltage (see the top section of figure 4). This situation does not allow the filament enough time to respond to the changing input voltage and thus the filament can only sense the mean (rms) voltage (represented by the horizontal broken lines). The top curves of figure 4 demonstrate that the calculated temperature of the filament (bold curves) coincides with the horizontal broken lines at high frequencies indicating that the filament does not have enough time to react to the voltage fluctuations.

Focusing on the middle plot of figure 4, near the frequency where the hysteresis is maximum, one sees that the asymmetry of the bold full curves with respect to the thin full curves is largest. This is the region where the thermal response time of the filament and
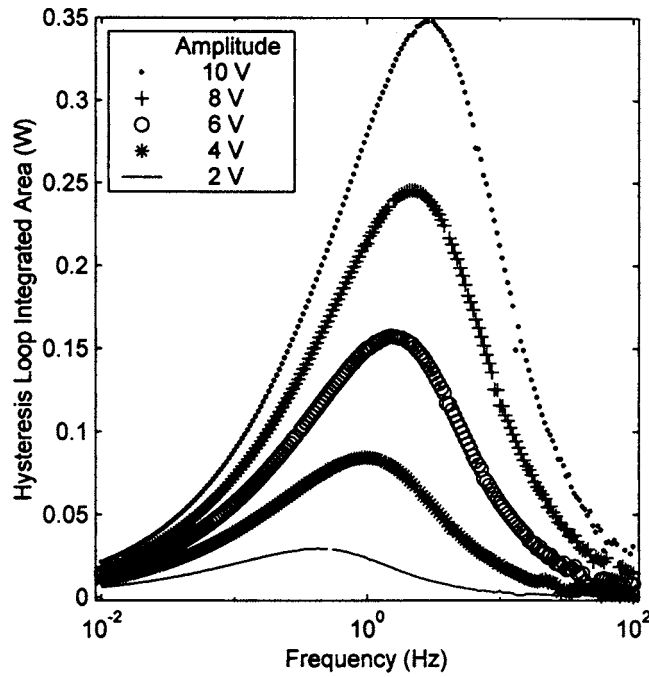
Figure 3. Integrated area of the hysteresis loops from calculated I–V curves for the bulb driven at various frequencies and amplitudes.

the driving period are comparable. Specifically, this figure indicates that the filament is still cooling ($dT/dt < 0$) even in regions where the voltage is increasing (where the slope of the thin lines is positive). Where the thin lines cross the bold lines, (dT/dt) switches sign and the filament temperature begins to rise. The cross-over points in figure 4 where (dT/dt) changes sign from negative to positive correspond to the elbows observed in the I–V curves of figure 1 where the voltage is increasing.

In addition to modelling dynamic circuit behaviour with alternating voltages, the model can also be used for steady-state conditions using constant voltages. Experimental I–V data are collected at 0.5 V increments in the range 2–10 V. These voltage and current measurements are then used to determine the filament resistance ($R = V/I$) at each steady-state temperature which are substituted into the following

$$R_0/R(T(V)) = \rho_0/\rho(T(V)) \tag{6}$$

which can be written in terms of a new function (F) as

$$F(T(V)) = \rho(T(V)) - \alpha R(T(V)) = 0 \tag{7}$$

where α is the ratio of the resistivity to the resistance at room temperature. The form of equation 7 allows one to use MatLab$^{©}$ at each input voltage to solve for $T(V)$. The results of this process are plotted in figure 5 as experimental data.

A similar virtual experiment is repeated using the model. Constant voltages are applied at 0.5 V increments in the model, which is run at each voltage until it converges to a steady-state temperature. The equilibrium temperature is then plotted versus the applied voltage. The results are plotted in figure 5 as calculated data. This steady-state model uses the same parameter values stated earlier for the dynamic version. However, when first calculated, the two datasets of figure 5 are parallel but not coincident. The only modification required to have the plots coincide as shown in figure 5 is the addition of systematic error terms, V_{err} and I_{err},
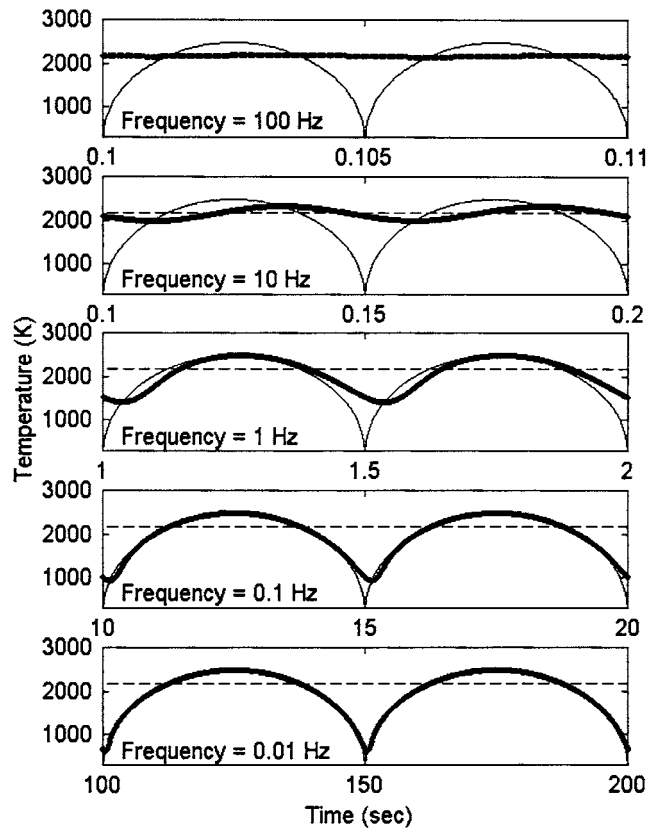
Figure 4. Numerical simulations of the filament temperature versus time using equation (5) (bold full curves) and approximate solutions to equation (5) with the rate-dependent term set to zero but the voltage kept time-dependent (thin full curves) or time-independent at the rms value (horizontal broken lines).

to the experimental voltage and current values. The systematic errors used to obtain figure 5 are $V_{err} = 20$ mV and $I_{err} = 4$ mA, which are acceptable considering the resolution of the test equipment used in this study.

Detailed studies of filaments under steady-state conditions can be found in the literature [7, 10] and the goal here is to validate that the dynamic model presented here predicts the correct dc limit. The steady-state behaviour reflected in figure 5 can be explained by considering that with a time-independent voltage source, and with the same simplifications used previously, equation (1) becomes

$$V^2/R(T) = e\sigma A_s T^4 \tag{8}$$

or, in simpler terms,

$$V^2 \propto R(T)T^4. \tag{9}$$

As mentioned previously, using the relationship [6, 8–10] $R \propto T^{1.2}$ yields $T \propto V^{0.38}$. A fit to the data of figure 5 yields $T \propto V^{0.39}$, in very good agreement with the dimensional analysis. This is a relatively simple analysis with respect to the dynamic modelling, and the experiment is much easier to perform. By measuring the steady-state current at various applied voltages, one can determine the filament temperature as a function of voltage using literature values for resistivity [17].
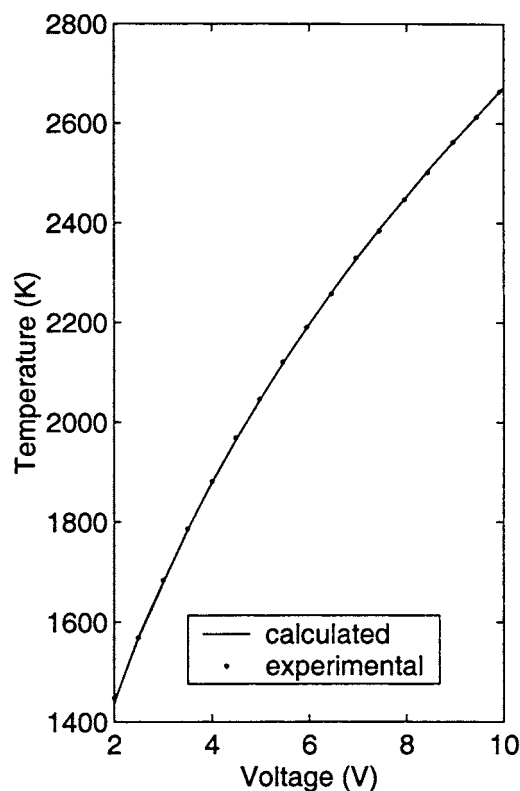
Figure 5. Measured and calculated values of the steady-state filament temperature versus applied dc voltage.

5. Extending this work

There are several ways to extend this work to arrive at a more detailed description of energy conversion phenomena. For example, a fraction of the light radiated by the bulb can be measured with a spectrally-integrating optical sensor. Preliminary data using a Pasco thermal radiation detector (TD-8553) indicate that the radiated power tracks the input electrical power, but with a time delay. This detector allows optical radiation passing through an aperture to be incident upon a broadband (blackbody) absorber that incorporates a thermopile to convert the incident energy into a voltage. There is a thermal time constant associated with transient measurements due to both the detector and the bulb. The thermal time constant of the detector could be determined by measuring its output with the bulb at constant voltage and then as a function of time as the detector is shielded and allowed to cool to room temperature. The effective thermal time constant of both the detector and bulb could be determined in a similar fashion, without shielding the detector but by removing the voltage from the bulb, and then the bulb time constant could be extracted and compared with other methods [8] for validation.

Another means of extending this work is by measuring the optical spectrum of the bulb in real time. Such spectra have been recorded, at 0.5 V intervals in the range 2–10 V after the bulb reaches steady-state conditions, with an Ocean Optics hand-held fibre-optic spectrometer (S2000) [22]. For each measurement, external light has to be avoided and the probe has to be moved to a distance from the bulb sufficient to ensure that the spectrometer does not saturate. The peak position of each spectrum is extracted from these data and the filament temperature at each voltage determined using the standard blackbody model. Qualitative agreement between

this method of measuring the filament temperature and that presented in the previous section using electrical resistance can be obtained. However, for both of these examples involving optical characterization, quantitative measurement of the total radiation from the bulb would have to incorporate an integrating sphere and/or considerations of the actual geometry and emissivity of the filament [6] and the geometry and spectral responsivity of the detectors.

The modelling could also be made more quantitative by incorporating the actual diameter of the filament, which will be non-uniform with respect to time due to evaporation [9] and thermal expansion [9]. The actual emissivity [15] of the filament could be incorporated in addition to considerations of the coiled geometry which causes radiation shielding [6]. Thermal conduction could be incorporated [15, 16], as could the fact that the glass envelope and bulb base do not behave as constant temperature sources of radiant flux back to the filament. Considerations of contact and lead resistance, the internal resistance of the power supply, and non-uniform current distribution in the filament could also be addressed, and may minimize the need for a systematic shift of the steady-state data. Another area of interest is to determine whether the model as it stands can reproduce the $I-V$ characteristics of bulbs of different types [14, 15] and power ratings and also those of bulbs driven with non-sinusoidal (e.g. square, triangle, sawtooth, etc) waveforms. In addition to integrated areas, other ways of analysing the hysteresis in the $I-V$ curves using slopes or curvatures might be revealing and a sensitivity analysis with respect to the values of e and L could be performed. Finally, the technique used to solve the differential equations could be modified, since it has been observed that the initial transient behaviour in the calculated results at high frequency does not reflect the measured data until dynamic equilibrium is reached.

6. Summary

A simple physical model has been shown to accurately reproduce the dynamic electrical response of a light bulb driven at various frequencies and amplitudes in addition to accounting for steady-state behaviour. Hysteresis, a phenomenon which occurs in many physical systems, has been observed and modelled. The approach uses commercially available hardware and software and can be easily adapted for a variety of educational purposes.

Acknowledgments

References

[1] Evans J 1978 Teaching electricity with batteries and bulbs *Phys. Teach.* **16** 15–22
[2] Steinberg M S and Wainwright C L 1993 Using models to teach electricity—the CASTLE project *Phys. Teach.* **31** 353–7
[3] McDermott L C and Shaffer P S 1992 Research as a guide for curriculum development: an example from introductory electricity. Part I: Investigation of student understanding *Am. J. Phys.* **60** 994–1003
McDermott L C and Shaffer P S 1993 Erratum **61** 81
[4] Shaffer P S and McDermott L C 1992 Research as a guide for curriculum development: an example from introductory electricity. Part II: Design of instructional strategies *Am. J. Phys.* **60** 1003–13
[5] Agrawal D C, Leff H S and Menon V J 1996 Efficiency and efficacy of incandescent lamps *Am. J. Phys.* **64** 649–54
[6] Leff H S 1990 Illuminating physics with light bulbs *Phys. Teach.* **28** 30–5

[7]   Edmonds I R 1968 Stephan–Boltzmann law in the laboratory *Am. J. Phys.* **36** 845–6

[8]   Menon V J and Agrawal D C 1999 Switching time of a 100 Watt bulb *Phys. Educ.* **34** 34–6

[9]   Agrawal D C and Menon V J 1998 Lifetime and temperature of incandescent lamps *Phys. Educ.* **33** 55–8
        Agrawal D C and Menon V J 1998 Incandescent bulbs: illuminating thermal expansion *Quantum* **8** 35–6

[10] Prasad B S N and Mascarenhas R 1978 A laboratory experiment on the application of Stefan's Law to tungsten
        filament electric lamps *Am. J. Phys.* **46** 420–3

[11] Zanetti V 1984 Sun and lamps *Am. J. Phys.* **52** 1127–30
        Zanetti V 1985 Temperature of incandescent lamps *Am. J. Phys.* **53** 546–8

[12] Kraftmakher Y 1995 Two student experiments on electrical fluctuations *Am. J. Phys.* **63** 932–5

[13] Yih S W H and Wang C T 1979 *Tungsten: Sources, Metallurgy, Properties, and Applications* (New York:
        Plenum) p 266–71

[14] Coaton J R and Marsden A M 1997 *Lamps and Lighting* (New York: Wiley) pp 161–9

[15] Elenbaas W 1972 *Light Sources* (London: Macmillan) pp 21–47

[16] Dow W G 1937 *Fundamentals of Engineering Electronics* (New York: Wiley) pp 206–9

[17] *CRC Handbook of Chemistry and Physics* 75th edn (Boca Raton, FL: CRC Press) pp 10–296

[18] See, for example, Mayergoyz I D 1991 *Mathematical Models of Hysteresis* (New York: Springer) pp xi–xx
        and 44–55

[19] Pasco Scientific, 10101 Foothills Blvd, PO Box 619011, Roseville, CA, 95661-9011, webpage www.pasco.com

[20] The Mathworks, Inc., 24 Prime Park Way, Natick, MA 01760, webpage www.mathworks.com

[21] 'Incandescent Lamps', Pamphlet TP-110R2 (Nela Park, General Electric Co., 1984)

[22] Ocean Optics, Inc., 1237 Lady Marian Lane, Dunedin, FL, 34698, webpage www.oceanoptics.com